Effect of Polarization on RF Signal Transmission over Two-Ray Channel

Srishti Sharma*, Chirantan Ganguly†, and Swades De*
*Department of Electrical Engineering and Bharti School of Telecommunication, IIT Delhi, New Delhi, India
†Institute of Radiophysics and Electronics, University of Calcutta, Kolkata, West Bengal, India

***Abstract*—This paper presents a practical two-ray model which accurately characterize the receiver power compared to conventional two-ray model for wireless communication and power transfer applications. The proposed model considers the impact of polarization orientations of line of sight (LOS) and non-line of sight (NLOS) components, and complex permittivity of the reflecting surface. On observing the received power for various different environmental settings (different source and receiver heights, transmission distance and reflector permittivity), it becomes apparent that the best suited polarization for maximum power reception alters between horizontal and vertical polarization in a single transmitter system. We show that when heights of transmitter and receiver and transmission distance are nearly same then vertical polarization provides relatively stable power. However, in arbitrary settings, for short range communication horizontal polarization is capable of delivering large power. We demonstrate that the over large communication distances, all polarization angles perform nearly identically. Additionally, we show theoretically that reflection may not only change orientation angle but may also alter the state of polarization of NLOS component.**

***Index Terms*—Polarization interference, reflector permittivity, RF energy transfer, short-range wireless communication, two-ray propagation channel**

I. Introduction

Future generation wireless networks are expected to deliver high data rates, massive connectivity, and enhanced reliability. To achieve these communication goals accurate channel modeling is required. A commonly used deterministic model for radio frequency (RF) communication and energy transfer is the Friis transmission equation [1]. It is applicable when the transmitter and receiver have a clear, unobstructed, and line-of-sight (LOS) path between them. However, practical radio channels never experience unobstructed communication since the nodes are nearer to the ground. Therefore, the multipath components caused due to reflections, refraction, and scattering in the environment should be accounted for, particularly at small transmission ranges when these multipath components are not significantly suppressed. These multipath components differ in amplitude, phase, and polarization causing the receiver power to fluctuate based on the constructive and destructive interference between the various multipath components. A study of the LOS link and an NLOS link individually and their interaction is a way to analyze the channel as its extension leads to a practical channel consisting of multipath components.

A. Related Works and Motivation

The performance of two-ray model has been investigated in many communication and network scenarios. The two-ray model discussed in [2] is suitable for outdoor environment where the effect of multipath is less because of long distance communication. However, the effect of NLOS component is strong in short-distance communication, hence its impact in the received signal must be examined. Authors in [3] analyzed a generalized two-ray model, consisting of two LOS and one diffused component, and derived the closed-form expression for moment generating function of signal-to-noise ratio. The work in [4] experimentally evaluated the two-ray model in near-shore scenario to predict the major trends of the path loss experienced by a 2.4 GHz over-water WiFi link. The authors in [5] demonstrate that the two-ray model is suitable for small-scale fading scenarios in mmWave communications and derived the break-point distance based on generalized first Fresnel zone. The work in [6] proposed a more exact two-ray propagation model for physical radio communication in Vehicular Ad Hoc Networks (VANETS) which also account for the imperfect reflections and the phase offset due to the path difference between the direct and reflected component.

Further, fluctuating two-ray (FTR) models are also proposed in literature wherein, the received signal consists of a diffused component along with the two specular components. Method of moments is used to estimate the parameters of FTR in [7]. Additionally, cascaded FTR channels [8], sum of squared two-ray random variables [9] and product of two-ray fluctuating random variates [10] are also proposed in literature for wireless applications.

However, none of the above works considered a crucial EM wave parameter, namely *polarization*, in developing the channel model for various scenarios. When an EM wave reflects from a surface, it is a well-known fact that its polarization is impacted by the reflector. Although the work in [11] does talk about polarization, the study is restricted to just horizontal and vertical polarization. Additionally, the study is limited to short-range energy transfer and did not account for the impact of various polarization angles for short as well as long-range communications. Therefore, a complete and precise model for received power needs to be developed which takes into account the various controllable parameters of EM wave, including polarization, to maximize the receive power.

In any mobile radio channel, signal propagation solely via direct LOS link is seldom. In general, the line of sight link is accompanied by one or more multipaths due to fading channel. In this work, we propose a generalized two-ray model which incorporates the effect of polarization in the transferred power through the LOS as well as NLOS (ground reflected) component. Moreover, we identify the signal polarization which would lead to a higher amount of received power in a given system setting and reflector surface; using this polarization based transmission strategy would help in further enhancing the received power. *To the best of our knowledge, this is the first work that report the studies of antenna polarization effects on two-ray propagation model.*

B. Contributions and Significance

The main contributions of this study are as follows:

1) An accurate two-ray channel model is proposed for characterizing the received power in wireless the scenario. This model incorporates the effect of polarization angles of source and receiver, and complex reflection coefficient of the reflection surface.
2) It is proven that the optimum polarization angle of the antennas (assuming both have the same orientation angles) is a strong function setup geometry (heights of transmitter and receiver, and separation distance between them) and permittivity of the reflecting surface.
3) It is observed that if communication distance is relatively equal to the transmitter and receiver heights, then the vertical polarization is capable of providing nearly stable power, whereas for horizontal polarization power fluctuates due to constructive and destructive phase interference between the LOS and NLOS link; the horizontal polarization is suitable as it provides larger received power levels.
4) It is observed that when the transmitter-receiver separation distance is larger than the critical distance (d_c) [2] then both the polarization angles perform nearly identically, and the difference in performance depends on the permittivity of the reflector.

The proposed two-ray channel model completes the study of the conventional two ray-model by accounting for the polarization of the NLOS component. This model can be applied in the study of FTR models or can be extended to the multipath scenario. The proposed model allows us to quantify the received power accurately in wireless communication and energy transfer applications [12], [13].

II. Proposed Two-Ray Channel Model

In this work, we consider a two-ray model where a LOS path is accompanied by a reflected path. Fig. 1 shows the system setup in which an RF source transmits a carrier signal to an RF receiver. The transmitter and receiver are at heights h_s and h_r respectively, placed L distance apart. Both source and receiver nodes are equipped with antennas to transmit and receive signals which are assumed to be plane-polarized. Polarization angles of transmit and receive antennas are indicated by α and β respectively, defined with respect to X in the XY plane. RF source is designated to send a signal to the receiver node, but due to obstacles present in indoor environment, it is accompanied by an NLOS component. We assume that the NLOS component is generated by a reflecting surface of relative permittivity ϵ_r. Since we are analyzing the impact of polarization of RF signal on the receiver power, we consider the analysis with the unmodulated carrier signal.

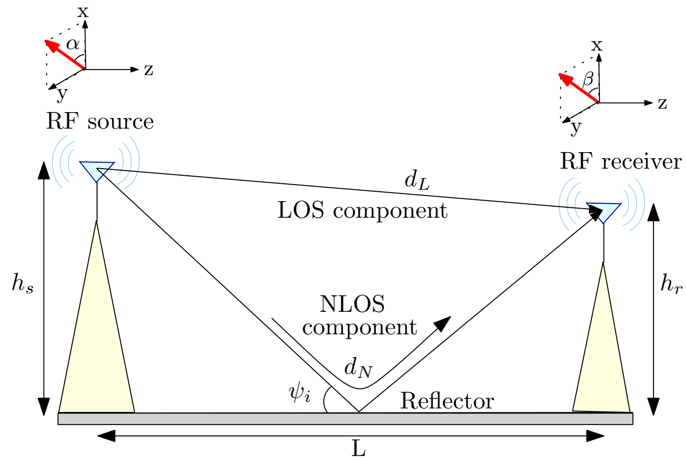

Fig. 1. System model accounting for source and receiver polarization in two-ray model.

As wireless communication and energy transfer applications are generally in far-field ($d_f > \frac{2D^2}{\lambda}$), where d_f denotes far-zone Fraunhofer distance, D is the largest dimension of the antenna and λ is the corresponding wavelength, we assume the electric field to be a plane wave. The generalized form of an electric field which emanates from an antenna is given by

$$\vec{E}(d,t) = \frac{E_o d_o}{d} e^{j(\frac{\pi}{\lambda}d - \omega t)} \hat{a}_e \quad (1)$$

where d_o is the reference distance at which the magnitude of the field is E_o, d is the distance at which the field is observed, ω is the angular frequency, and $\hat{a}_e$ denotes the polarization of the field.

Friis transmission equation [14], [15] relates the transmitted power to the receiver power in the far field by inverse square law of distance and is given by

$$\begin{aligned} P_r^{Friis} =& P_t G_t(\theta_t,\phi_t) G_r(\theta_r,\phi_r)(1-|\Gamma_t|^2)(1-|\Gamma_r|^2) \\ & \times \left(\frac{\lambda}{4\pi d}\right)^2 |\hat{a}_e . \hat{a}_r|^2. \end{aligned} \quad (2)$$

Here P_t represents the transmit power, G_t and G_r respectively denote the gains of transmit and receive antennas in elevation (θ_r, θ_t) and azimuth (ϕ_r, ϕ_t) directions, Γ_t and Γ_r are the transmitter and receiver reflection coefficients due to mismatch between their corresponding antennas and load. The term $|\hat{a}_e . \hat{a}_r|^2$ denotes the polarization loss factor (PLF) which accounts for the polarization mismatch between the transmitter and receiver antennas. From Friis transmission equation we deduce that to maximize the receiver power the PLF should be

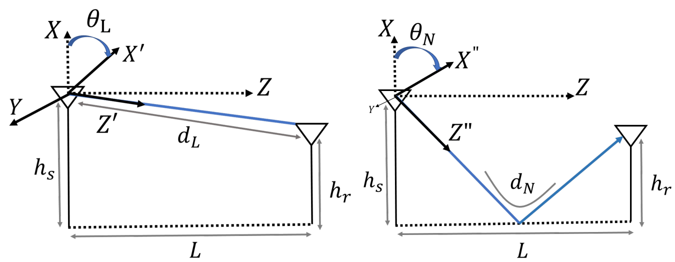

(a) (b)

Fig. 2. Illustration depicting the translation of coordinate system for (a) LOS component, (b) NLOS component.

close to 1. However, it does not investigate the effect of NLOS component which is invariably present in practical settings.

Next, we derive the expression for LOS and NLOS components and the generalized expression for total received power for the proposed two-ray channel model.

A. LOS and NLOS Field Components

The power at a certain distance d from the transmitting antenna is related to the electric field $\vec{E}$ at that distance d as

$$P_t(d) = |\vec{E}(d)|^2/\eta \tag{3}$$

where η is the intrinsic impedance of free space. From (2) and (3), the magnitude of E-field reaching the receiver antenna directly through LOS connectivity is given by

$$\vec{E}_L(d_L, t) = \Re\left\{\sqrt{\frac{P_t}{4\pi d_L^2} G_{tL}(1-\Gamma_t^2)\eta} e^{j\left(\omega t - \frac{2\pi d_L}{\lambda}\right)} \hat{a}_L\right\} \tag{4}$$

where θ_L is the angle of arrival of the LOS ray at the receiving antenna as shown in Fig. 2(a), G_{tL} is the gain associated with LOS link and d_L is the length of LOS link. $\hat{a}_L$ denotes the polarization vector for LOS ray which is obtained by rotating the polarization vector in XYZ to $X'YZ'$ coordinate system as shown in Fig. 2(a). Therefore, the polarization vector for LOS link is given by

$$\begin{aligned}\hat{a}_L &= \begin{bmatrix}\cos\alpha\\ \sin\alpha\\ 0\end{bmatrix}^T \begin{bmatrix}\cos(-\theta_L) & 0 & -\sin(-\theta_L)\\ 0 & 1 & 0\\ \sin(-\theta_L) & 0 & \cos(-\theta_L)\end{bmatrix}\\ &= \cos\alpha\cos\theta_L\hat{a}_x + \sin\alpha\hat{a}_y + \cos\alpha\sin\theta_L\hat{a}_z.\end{aligned} \tag{5}$$

As antenna gain varies with elevation and azimuthal coordinates, the impact of reflected component depends on the antenna gain in that direction. The reflected component alters the effective field at the receiver. It may add constructively or destructively to the LOS component depending on their relative phase and polarization angles. The NLOS ray before reflection can be written as

$$\vec{E}_N(d', t) = \Re\left\{\sqrt{\frac{P_t}{4\pi d'^2} G_{tN}(1-\Gamma_t^2)\eta} e^{j\left(\omega t - \frac{2\pi}{\lambda} d'\right)} \hat{a}'_N\right\}. \tag{6}$$

Here G_{tN} is the transmitter antenna gain in NLOS direction, d' is the distance between the source and the point of reflection and θ_N is the angle which NLOS ray makes with the X-axis as shown in Fig. 2(b). Polarization vector for NLOS component is derived similarly as for LOS component in (5), by translating the vector from XYZ coordinate system to $X''YZ''$ as shown in Fig. 2(b) which is given by

$$\hat{a}_N^{'} = (\cos\alpha\cos\theta_N\hat{a}_x + \sin\alpha\hat{a}_y + \cos\alpha\sin\theta_N\hat{a}_z). \tag{7}$$

Upon reflection from a complex surface the NLOS ray may undergo amplitude, phase and polarization change. Therefore, the reflected NLOS component is expressed as

$$\vec{E}_N(d_N, t) = \Re\left\{\sqrt{\frac{P_t}{4\pi d_N^2} G_{tN}(1-\Gamma_t^2)\eta} e^{j\left(\omega t - \frac{2\pi}{\lambda} d_N\right)} \hat{a}_N\right\} \tag{8}$$

where d_N is the total length of the NLOS component as shown in Fig. 2(b). From the geometry of Fig. 1, the length d_N is calculated as

$$d_N = \sqrt{h_s^2 + \left(\frac{h_s L}{h_s + h_r}\right)^2} + \sqrt{h_r^2 + \left(\frac{h_r L}{h_s + h_r}\right)^2}. \tag{9}$$

The polarization vector of NLOS component is modified after reflection, given by

$$\begin{aligned}\hat{a}_N &= \Gamma_{\parallel}\cos\alpha\cos\theta_N\hat{a}_x + \Gamma_{\perp}\sin\alpha\hat{a}_y\\ &\quad - \Gamma_{\parallel}\cos\alpha\sin\theta_N\hat{a}_z\end{aligned} \tag{10}$$

where $\Gamma_{\parallel} = |\Gamma_{\parallel}|e^{j\varphi_{\parallel}}$ and $\Gamma_{\perp} = |\Gamma_{\perp}|e^{j\varphi_{\perp}}$ respectively denote Fresnel reflection coefficients for parallel and perpendicular polarization. It should be noted that both $\Gamma_{\parallel}$ and $\Gamma_{\perp}$ are functions of incidence angle ψ_i, and permittivity of reflecting surface ϵ_r. and are expressed as [16]

$$\Gamma_{\parallel} = \frac{-\epsilon_r\sin(\psi_i) + \sqrt{\epsilon_r - \cos^2(\psi_i)}}{\epsilon_r\sin(\psi_i) + \sqrt{\epsilon_r - \cos^2(\psi_i)}}, \tag{11}$$

$$\Gamma_{\perp} = \frac{\sin(\psi_i) - \sqrt{\epsilon_r - \cos^2(\psi_i)}}{\sin(\psi_i) + \sqrt{\epsilon_r - \cos^2(\psi_i)}}. \tag{12}$$

From (11) and (12), we observe that if ϵ_r is real, then the reflection coefficients obtained are real, otherwise complex.

Remark *1: If the permittivity of the reflector is real valued, then only polarization orientation of NLOS component changes whereas if the reflector permittivity is complex valued then the state of polarization of the reflected NLOS component may also change.*

Now based on the source polarization and the complex relative permittivity of the reflecting surface, the polarization of the LOS and NLOS components will vary. Therefore, from here we conclude that not only relative phase, but relative polarization mismatch between the LOS and NLOS components also affect the receiver power. However, since the NLOS component incurs additional losses due to antenna gain, ground reflection and propagation, the effect of NLOS component is not very drastic to cause complete destructive interference at the receiver.

B. Total Received Power

Total electric field at the receiver antenna is given by

$$\vec{E}_T = \vec{E}_L + \vec{E}_N. \tag{13}$$

The effective vector height of the receiving antenna is given by [11]

$$\vec{H}_{eff} = \left(\sqrt{(1 - \Gamma_r^2) \frac{\lambda^2}{4\pi} G_r(\theta, \phi)} \right) \hat{a}_{rx} \tag{14}$$

where $\hat{a}_{rx} = \cos\beta\hat{a}_x + \sin\beta\hat{a}_y$ is the polarization vector of the receiver antenna. The combined power due to LOS and NLOS components at the receiver antenna is expressed as

$$P_r = (\vec{E}_T \cdot \vec{H}_{eff})^2/\eta. \tag{15}$$

Since $G_r(\theta, \phi)$ is a function of angle of arrival, it will take different values for LOS and NLOS component. We express the directional gains for LOS and NLOS components as G_{rL} and G_{rN}, respectively. Substituting the values from (4), (8), (13) and (14) in (15), we obtain the total power at the receiver antenna as given in (16). It represents the generalized two-ray model equation which includes the effects of the random polarization of the transmitters and receivers and also holds good for any real or complex reflecting surface. It should be noted that for $\alpha = 0$ and $\alpha = \frac{\pi}{2}$, (16) reduces to the two-ray model given in [11] thereby validating our proposed model.

The main motivation behind investigating the two-ray model here is that, it is the most fundamental path loss model to account for the contribution of reflected ray and is found to be fairly accurate in predicting the signal power over kilometers for RF systems [16].

III. Results and Discussion

In this section, we analyze the derived generalized two-ray model incorporating the polarization effects using MATLAB simulations. Since LOS component carries the majority of the power, we keep the polarization angles of the transmitter and the receiver antenna equal, (i.e., $\alpha = \beta$) during computations of the results to minimize the cross-polarization loss from the antennas. For simulation, the transmitter power is taken to be 10 dBm and the operating frequency is 2 GHz. The analytical expression for gain of omnidirectional antenna is taken to be $G(\theta, \phi) = G_{om} \sin^2(\theta)$ [11]. The range of angles traversed by the azimuth plane and elevation plane are $\phi \in [0 \;\; 2\pi]$ and $\theta \in [0 \;\; \pi]$ and G_{om} is taken to be 3 dBi.

***Remark** 2: The terms "horizontal" ($\alpha = \frac{\pi}{2}$) and "vertical" ($\alpha = 0$) refer to polarization vectors that are respectively perpendicular and parallel to the plane in which the source, receiver, and reflector are located.*

***Note** 1:* At RF frequencies the imaginary part of the relative permittivity is very small for most of the substances. Therefore, to compare to the practical environment scenario we have used real permittivity values. However, the analysis carried out in Section II is general and applicable to reflectors with real as well as complex permittivity values.

From (16) we observe that the power received by the antenna is function of channel length (L), source height (h_s), receiver height (h_r), polarization angle (α and β) and also permittivity of the reflector (ϵ_r). In the following subsections, we analyze the impact of above stated parameters on the received power.

A. Effect of Permittivity of Reflector on Fresnel Coefficients

Fig. 3(a) shows the variation of reflection coefficient with the incidence angle for two different permittivity values. We observe that irrespective of the permittivity value, $|\Gamma_\perp| \geq |\Gamma_\parallel|$ always. We note that for low incidence angles, the difference between the parallel and perpendicular reflection coefficient is large and this difference decreases with an increase in incidence angles. Also, it can be noticed that Fresnel coefficients are typically high for materials with high permittivity. Here and in the discussion ahead we consider two permittivity values with $\epsilon_r = 5$ and 70 which roughly correspond to the most common reflectors in the environment, namely wood and water respectively at the considered frequency.

B. Effect of Polarization on Received Power

Fig. 3(b) and 3(c) show the variation in power levels for different polarization angles. It is observed that all three polarization angles act identically with varying LOS (d_L) and NLOS (d_N) link lengths. Hence, we conclude that for two-ray model analysis with either horizontal polarization or vertical polarization is sufficient as they respectively form the upper and lower bound for all other polarization angles. Therefore, in the discussion ahead we will only consider the two extreme polarization angles, i.e., $\alpha = 0$ and $\pi/2$.

C. Effect of Transmitter Height on Received Power

From Fig. 3(b) we observe that the vertical ($\alpha = 0$) polarization suffers less oscillation compared to $\alpha = \frac{\pi}{2}$, when the transmitter and receiver heights are on the order of communication distance (i.e., all three are nearly equal). This is because at α close to zero, received power nearly becomes independent of $|\Gamma_\perp|$ and hence the small variation are due to the effect of $|\Gamma_\parallel|$, which is small compared to $|\Gamma_\perp|$. When the transmitter height is increased, performance is similar to the conventional two-ray model [16], as the LOS and NLOS link lengths nearly become equal as shown in Fig. 3(c). This convergence to the conventional two-ray model also validates our analysis. However, it is notable that the power received for different polarization angles are different. This is due to the large difference in the Fresnel coefficients of reflector surface for small values of ψ_i, $\psi_i \neq 0$. Hence, for long-distance communication, horizontal polarization is more suitable as it can comparatively provide larger power levels.

D. Effect of Transmitter-Receiver Separation Distance on Received Power

To analyze the impact of transmitter-receiver separation distance on receiver, we divide the propagation distance L in four ranges as given below:

1) $L \leq h_s$ and h_r: In this range, effect of the NLOS component on the received power is negligible, thereby

$$P_R = P_t(1-\Gamma_t^2)(1-\Gamma_r^2)\left(\frac{\lambda}{4\pi}\right)^2 \Bigg[\frac{G_{tL}G_{rL}}{d_L^2}\left(\cos\alpha\cos\beta\frac{L}{d_L}+\sin\alpha\sin\beta\right)^2 + \frac{G_{tN}G_{rN}}{d_N^2}\Bigg\{\left(\Gamma_\parallel\cos\alpha\cos\beta\frac{L}{d_N}\right)^2$$
$$+\ (\Gamma_\perp\sin\alpha\sin\beta)^2 + 0.5\Gamma_\parallel\Gamma_\perp\sin 2\alpha\sin 2\beta\cos(\varphi_\parallel-\varphi_\perp)\Bigg\} + \frac{\sqrt{G_{tL}G_{rL}G_{tN}G_{rN}}}{d_Ld_N}\left(\cos\alpha\cos\beta\frac{L}{d_L}+\sin\alpha\sin\beta\right)$$
$$\times 2\left\{\frac{L}{d_N}\Gamma_\parallel\cos\alpha\cos\beta\cos\left(\frac{2\pi}{\lambda}(d_N-d_L)-\varphi_\parallel\right)+\Gamma_\perp\sin\alpha\sin\beta\cos\left(\frac{2\pi}{\lambda}(d_N-d_L)+\varphi_\perp\right)\right\}\Bigg]. \quad (16)$$

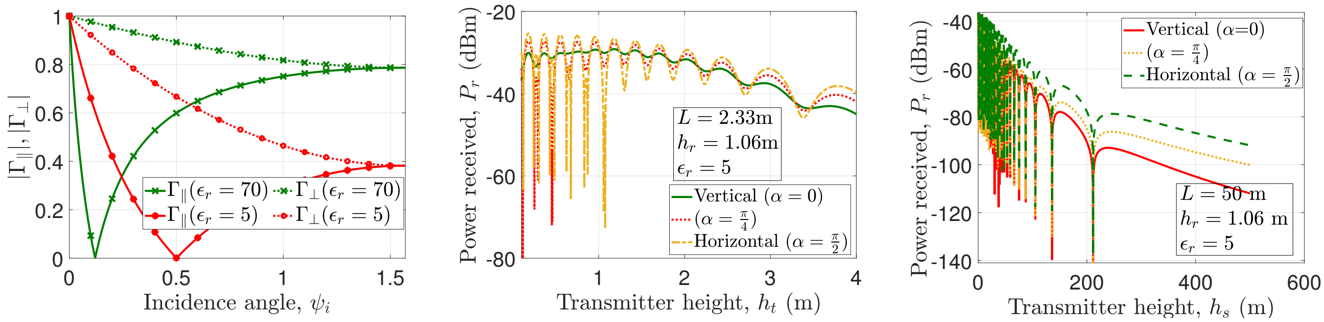

(a) (b) (c)

Fig. 3. (*a*) Variation of Fresnel reflection coefficients with incidence angles. (*b*) Received power for various heights of transmitter antenna for $L = 2.33$ m. (*c*) Received power for various heights of transmitter for $L = 50$ m.

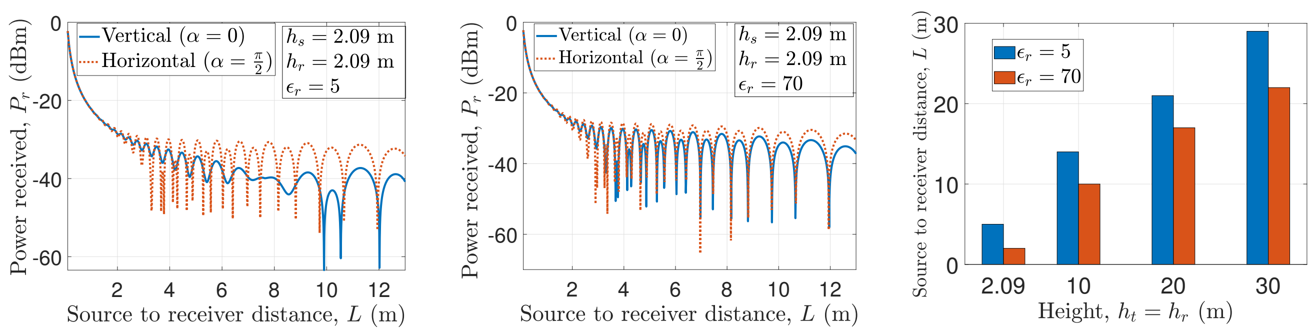

(a) (b) (c)

Fig. 4. (*a*) Received power versus transmission length for $\epsilon_r = 5$. (*b*) Received power versus transmission length for $\epsilon_r = 70$. (*c*) Transmission distance up to which near stable power for vertical polarization is received for various heights of transmitter antenna.

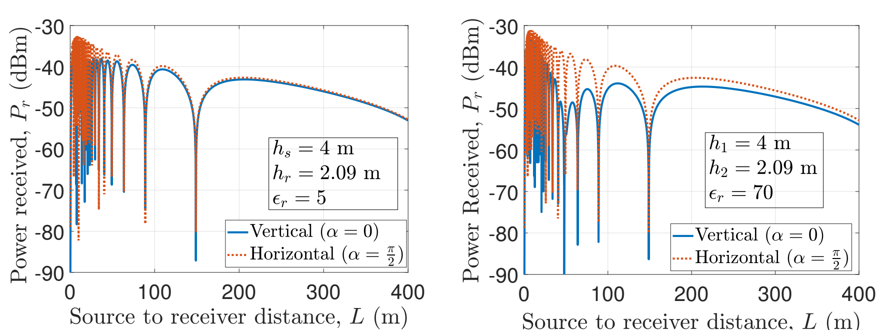

(a) (b)

Fig. 5. Transmission over long distances for (*a*) $\epsilon_r = 5$, (*b*) $\epsilon_r = 70$.

delivering constant power to the receiver as only LOS component is present as shown in Fig. 4(a) and 4(b).

2) $L \approx h_s$ and h_r: As discussed in Section III-C, vertical polarization suffers less oscillation due to the small value of $\Gamma_{\parallel}$. This can be observed in Fig. 4(a) and 4(b) as well. Fig. 4(c) shows the graph which indicates the transmission distances up to which the vertical polarization shows less oscillation compared to the horizontal polarization. It can be observed that this length is approximately equal to the heights of the antennas and decreases with increasing permittivity of the reflector.
3) h_s and $h_r \leq L \leq d_c$: Here, $d_c = \frac{4h_s h_r}{\lambda}$ is the critical distance [2]. In this channel range both polarization angles fluctuate due to constructive and destructive interference nearly identically. However, horizontal polarization performs slightly better than the vertical. This is due to polarization synchronization between the LOS and NLOS components and the large value of $|\Gamma_{\perp}|$ compared to $|\Gamma_{\parallel}|$.
4) $L \geq d_c$: At large distances (large compared to heights of transmitter and receiver) the received power is nearly identical for both the polarization angles because when $\psi_i \approx 0$, $\Gamma_{\parallel} \approx \Gamma_{\perp} \approx 1$, therefore both the components are identically affected and the effect of surface permittivity fades away as shown in Fig. 5(a) and 5(b). Also, if directional antennas are used then the gain of the NLOS component is low compared to the LOS component, then at $L \geq d_c$, NLOS component does not contribute significantly to the received power levels. Thus, both the polarization angles perform identically. In such settings Friis transmission equation gives very less error compared to the proposed model.

E. Effect of Permittivity on Received Power

From Fig. 4(a), we observe that over short-distance communication, i.e., when ψ_i is large, the difference between $|\Gamma_{\perp}|$ and $|\Gamma_{\parallel}|$ is large for small permittivity values, thereby causing the large difference in received powers of horizontal and vertical polarization angles. On the other hand, for large permittivity reflectors difference between powers for horizontal and vertical polarization is small as shown in Fig. 4(b). However, for long-distance communication, when ψ_i is small all the polarization angles perform nearly identically. Since ψ_i is not very small, difference between $|\Gamma_{\perp}|$ and $|\Gamma_{\parallel}|$ is large for large permittivity values, causing the received power for vertical and horizontal polarization to differ as shown in Fig. 5(b).

Therefore, in the two-ray model presented in this work, horizontal polarization performs better in terms of received power due to large value of $|\Gamma_{\perp}|$ and polarization matching between LOS and NLOS components.

IV. Conclusion and Future Scope

In this work, we proposed a generalized two-ray model for accurate quantification of the receiver power for RF communication and on-demand energy transfer. The proposed model highlights the impact of polarization and permittivity of reflector on the receiver power. Based on mathematical derivation and analytical results, we conclude that there is a strong interplay between the transmitter-receiver heights, their separation distance, their polarization, and permittivity of the reflectors on the overall received power. Additionally, we noted that in short-range communications, such as indoor environments, polarization orientation of the transmitted signal plays an important role, whereas, at a longer source-receiver distance, such as outdoor environments, the polarization orientation has very little impact. In future work, the proposed model will be verified for the short-and long-distance communications using experiments and will be extended to multipath channel fading scenarios for increased accuracy.

V. Acknowledgement

This work has been supported in parts by DST-SERB grant CRG/2019/002293, Abdul Kalam Technology Innovation National Fellowship, and Prime Minister's Research Fellows scheme.

References

[1] C. Balanis, *Antenna theory: analysis and design*. John Wiley & Sons, Dec. 2015.

[2] A. Goldsmith, *Wireless communications*. Cambridge university press, Aug. 2005.

[3] M. Rao, F. J. Lopez-Martinez, M.-S. Alouini, and A. Goldsmith, "MGF approach to the analysis of generalized two-ray fading models," *IEEE Trans. Commun.*, vol. 14, no. 5, pp. 2548–2561, Jan 2015.

[4] M. G. Gaitán, P. M. Santos, L. R. Pinto, and L. Almeida, "Experimental evaluation of the two-ray model for near-shore WiFi-based network systems design," in *IEEE Vehicular Technology Conference (VTC2020-Spring)*, May 2020, pp. 1–3.

[5] E. Zöchmann, K. Guan, and M. Rupp, "Two-ray models in mmWave communications," in *IEEE International Workshop on Signal Processing Advances in Wireless Communications (SPAWC)*, Jul 2017, pp. 1–5.

[6] C. Sommer and F. Dressler, "Using the right two-ray model? A measurement based evaluation of PHY models in VANETs," in *Proc. ACM MobiCom*, Sep. 2011, pp. 1–3.

[7] B. Shi, L. Pallotta, G. Giunta, C. Hao, and D. Orlando, "Parameter estimation of fluctuating two-ray model for next generation mobile communications," *IEEE Trans. Veh. Technol.*, vol. 69, no. 8, pp. 8684–8697, Jun 2020.

[8] O. S. Badarneh and D. B. da Costa, "Cascaded fluctuating two-ray fading channels," *IEEE Commun. Lett.*, vol. 23, no. 9, pp. 1497–1500, Jul 2019.

[9] J. Zheng, J. Zhang, G. Pan, J. Cheng, and B. Ai, "Sum of squared fluctuating two-ray random variables with wireless applications," *IEEE Trans. Veh. Technol.*, vol. 68, no. 8, pp. 8173–8177, Jun 2019.

[10] O. S. Badarneh, D. B. da Costa, M. Benjillali, and M.-S. Alouini, "Ratio of products of fluctuating two-ray variates," *IEEE Commun. Lett.*, vol. 23, no. 11, pp. 1944–1948, Aug. 2019.

[11] S. Kumar, S. De, and D. Mishra, "RF energy transfer channel models for sustainable IoT," *IEEE Internet Things J.*, vol. 5, no. 4, pp. 2817–2828, Apr. 2018.

[12] D. Mishra, S. De, and C.-F. Chiasserini, "Joint optimization schemes for cooperative wireless information and power transfer over Rician channels," *IEEE Trans. Commun.*, vol. 64, no. 2, pp. 554–571, Dec. 2016.

[13] I. Krikidis, S. Timotheou, S. Nikolaou, G. Zheng, D. W. K. Ng, and R. Schober, "Simultaneous wireless information and power transfer in modern communication systems," *IEEE Commun. Mag.*, vol. 52, no. 11, pp. 104–110, Nov. 2014.

[14] S. Suman and S. De, "Optimal UAV-aided RFET system design in presence of hovering inaccuracy," *IEEE Trans. Commun.*, Sep. 2021.

[15] P. Nintanavongsa, U. Muncuk, D. R. Lewis, and K. R. Chowdhury, "Design optimization and implementation for RF energy harvesting circuits," *IEEE J. Emerg. Sel.*, vol. 2, no. 1, pp. 24–33, Feb. 2012.

[16] T. S. Rappaport *et al.*, *Wireless communications: principles and practice*. prentice hall PTR New Jersey, 1996, vol. 2.